

## Article

# Zirconium(IV) Metal Organic Frameworks with Highly Selective Sorption for Diclofenac under Batch and Continuous Flow Conditions

Anastasia D. Pournara <sup>1</sup>, Evangelos K. Andreou <sup>2</sup> , Gerasimos S. Armatas <sup>2</sup>  and Manolis J. Manos <sup>1,3,\*</sup> 

<sup>1</sup> Department of Chemistry, University of Ioannina, 45110 Ioannina, Greece; anastasiapournara@gmail.com

<sup>2</sup> Department of Materials Science and Technology, University of Crete, 70013 Heraklion, Greece; vaggelisandr@gmail.com (E.K.A.); garmatas@materials.uoc.gr (G.S.A.)

<sup>3</sup> Institute of Materials Science and Computing, University Research Center of Ioannina, 45110 Ioannina, Greece

\* Correspondence: emanos@uoi.gr

**Abstract:** Diclofenac (DCF) is among the most effective non-steroidal anti-inflammatory drugs (NSAIDs) and at the same time one of the most consumed drugs worldwide. Since the ever-increasing use of diclofenac poses serious threats to ecosystems, its substantial removal is crucial. To address this issue, a variety of sorbents have been employed. Herein we present the diclofenac removal properties of two metal organic frameworks, namely  $[\text{Zr}_6\text{O}_4(\text{OH})_4(\text{NH}_2\text{BDC})_6] \cdot x\text{H}_2\text{O}$  (**MOR-1**) and  $\text{H}_{16}[\text{Zr}_6\text{O}_{16}(\text{H}_2\text{PATP})_4] \cdot x\text{H}_2\text{O}$  (**MOR-2**). Batch studies revealed fast sorption kinetics for removal of  $\text{DCF}^-$  from water as well as particularly high selectivity for the drug vs. common competitive species. Moreover, the composite **MOR-1**-alginate material was utilized in a sorption column, displaying remarkable removal efficiency towards  $\text{DCF}^-$  anions. Significantly, this is the first time that column sorption data for removal of NSAIDs using MOF-based materials is reported.

**Keywords:** diclofenac sodium; metal-organic frameworks; column study; environmental pollution; water remediation; non-steroidal anti-inflammatory drug (NSAID); pharmaceutical pollutants



**Citation:** Pournara, A.D.; Andreou, E.K.; Armatas, G.S.; Manos, M.J.

Zirconium(IV) Metal Organic Frameworks with Highly Selective Sorption for Diclofenac under Batch and Continuous Flow Conditions. *Crystals* **2022**, *12*, 424. <https://doi.org/10.3390/cryst12030424>

Academic Editor: Paul R. Raithby

Received: 4 March 2022

Accepted: 16 March 2022

Published: 18 March 2022

**Publisher's Note:** MDPI stays neutral with regard to jurisdictional claims in published maps and institutional affiliations.



**Copyright:** © 2022 by the authors. Licensee MDPI, Basel, Switzerland. This article is an open access article distributed under the terms and conditions of the Creative Commons Attribution (CC BY) license (<https://creativecommons.org/licenses/by/4.0/>).

## 1. Introduction

Access to clean freshwater represents a challenge not only for developing countries but also for the developed world. The rapid urbanization and the improved standards of living along with escalating demands in the prevention and treatment of human diseases has led to an increase in the production and the use of pharmaceutical products [1–3]. Pharmaceuticals are emerging pollutants [4,5], which access the water stream via excretion, once they have completed their role in body systems, having aquatic ecosystems as their final destination. These compounds represent a unique category of pollutants as they are not passive but rather, they are bioaccumulated, sustained, and toxic to living organisms [6]. Among these pharmaceuticals, diclofenac (Figure 1) is classified as an emerging micropollutant. Diclofenac is extensively used as a non-steroidal anti-inflammatory drug (NSAID) and is commonly found in the form of carboxylate anions ( $\text{pK}_a \sim 4$ ) in surface and ground water as well as in drinking water [7–10]. Therefore, the removal of this emerging contaminant from our potable water and aquatic resources is becoming an important issue [11]. So far, various conventional methods, including coagulation–flocculation [12], biodegradation [13,14], photodegradation [15], chlorination [16], and sorption [17–19], have been adopted to remove pharmaceuticals from aquatic ecosystems. Among them, sorption is considered as a promising method considering its cost efficiency, ease operation, and low energy consumption [4,20]. The main challenge of the sorption is the development and selection of suitable sorbents. Up to now, carbonaceous materials including activated carbons (ACs) have been used widely for the removal of such pollutants from water, owing to their high surface area and relatively low price [21,22]. Moreover, other sorbents such as MCM-41 [23],

SBA-15 [11], amberlite XAD-7 [24], and bentonite [25], have also been studied. Since most traditional sorbents still suffer from considerable limitations in real world applications, such as low sorption capacity, slow kinetics and short life cycles, researchers are looking for novel materials with superior sorption properties.

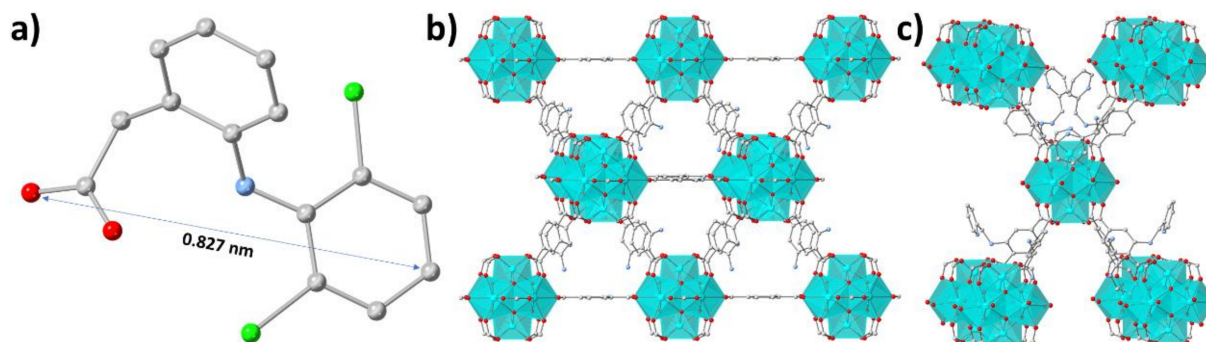


**Figure 1.** Representation of the structures of (a) diclofenac sodium salt, (b) MOR-1 and (c) MOR-2. Color code: C, grey; Cl, green; O, red; N, blue; Zr, cyan.

Among known sorbents, metal organic frameworks (MOFs) have recently attracted significant interest as they combine high porosity, tunable chemical composition, a variety of functional groups, etc. [26–28]. The reported studies on the capture of NSAIDs by MOFs have been focused on batch sorption investigations, which in most cases are incomplete [29–35]. For example, sorption data in the presence of competitive ionic species have not been included for most studied MOFs and, thus, the performance of MOF sorbents under realistic conditions is largely unknown. In addition, practical wastewater remediation requires treatment under continuous flow [36]. Till now, to the best of our knowledge, there are no investigations on MOFs for removal of pharmaceuticals under such conditions.

Our group has reported two MOFs,  $[\text{Zr}_6\text{O}_4(\text{OH})_4(\text{NH}_2\text{BDC})_6] \cdot x\text{H}_2\text{O}$  (**MOR-1**) and  $\text{H}_{16}[\text{Zr}_6\text{O}_{16}(\text{H}_2\text{PATP})_4] \cdot x\text{H}_2\text{O}$  (**MOR-2**) ( $\text{NH}_2\text{-H}_2\text{BDC}$  = 2-amino-terephthalic acid;  $\text{H}_2\text{PATP}$  = 2-((pyridin-1-ium-2-ylmethyl)ammonio)terephthalate) (Figure 1) [37,38], which have shown excellent sorption properties for inorganic anions and anionic dyes because of their facile anion binding properties.

Here, we report on the diclofenac anion ( $\text{DCF}^-$ ) capture properties of **MOR-1** and **MOR-2**. These MOFs have shown quite fast sorption for removal of  $\text{DCF}^-$  from water as well as particularly high selectivity for the drug vs. common competitive anions. The excellent  $\text{DCF}^-$  sorption properties of **MOR-1** and **MOR-2** are due to the strong interactions of the drug with the framework of the MOFs. In addition, for the first time we present here column sorption data for removal of NSAIDs using MOF-based materials. Specifically, the composite form of **MOR-1** with alginic acid (HA) mixed with silica sand was utilized as the stationary phase in the sorption column, which has shown capability for quantitative removal of  $\text{DCF}^-$  from water as well as reusability. These results point toward the practical utilization of MOFs for wastewater treatment applications related to removal of pharmaceuticals.

## 2. Materials and Methods

### 2.1. Materials

All reagents and solvents were purchased from Alfa-Aesar or Sigma-Aldrich and used as received. The water used was purified through a Millipore system.

### 2.2. Syntheses

The syntheses of **MOR-1/MOR-1-HA** as well as **MOR-2** materials were reported previously by us (references [37,38], respectively).

### 2.3. Physical Measurements

Powder X-ray diffraction measurements were carried out on a Bruker D2-Phaser X-ray diffractometer (CuK $\alpha$  radiation source, wavelength = 1.54184 Å). Unit cell indexing and Le Bail refinement data were performed using TOPAS [39]. ATR-IR spectra were collected in the range of 4000–400 cm<sup>-1</sup> using an Agilent Cary 630 FTIR photometer. DCF<sup>-</sup> determination regarding the sorption experiments was performed by UV-vis spectroscopy with an Agilent Cary 60 UV-vis spectrophotometer from 200 to 800 nm. Scanning Electron Microscope (SEM) images were recorded on a JEOL JSM6390LV SEM. N<sub>2</sub> adsorption-desorption isotherms were determined at 77 K on a Quantachrome Nova 3200e sorption analyzer. The activation of the samples involved EtOH-exchange, supercritical CO<sub>2</sub> drying, and then degassing at 393 K under vacuum (<10<sup>-5</sup> Torr) for 12 h. The specific surface areas were estimated using the Brumauer-Emmett-Teller (BET) method for the isotherm data in the 0.05–0.25 relative pressure (P/P<sub>0</sub>) range. Zeta potential was evaluated with a Malvern Zetasizer Nano ZS (Malvern Panalytical, Worcestershire, UK).

### 2.4. Batch DCF<sup>-</sup> Sorption Studies

The isolation of MOFs loaded with DCF<sup>-</sup> was performed as following: **MOR-1** or **MOR-2** (~0.04 mmol) was treated with a solution of diclofenac sodium (C<sub>0</sub> = 195 ppm; 0.61 mmol) in water (10 mL, pH ~7), under magnetic stirring for ~20 min. Then, the solids were isolated by filtration, washed several times with water and acetone, and dried in the air. The DCF<sup>-</sup> uptake from solutions with concentrations in the range 50–5000 ppm was studied by the batch method at V:m ~1000 mL/g, room temperature, and 10 min contact. DCF<sup>-</sup> analysis was undertaken via UV-Vis and the obtained data were used for the determination of DCF<sup>-</sup> sorption isotherms. The competitive sorption experiments were conducted with DCF<sup>-</sup> solutions containing Cl<sup>-</sup>, NO<sub>3</sub><sup>-</sup>, and SO<sub>4</sub><sup>2-</sup> with concentrations from 6.5 to 650 mM. This study was also performed with the batch method at V:m ratio ~1000 mL/g, room temperature, and 10 min contact. The sorption kinetics were determined via DCF<sup>-</sup> sorption experiments of various reaction times (1–60 min). For each experiment, a 10 mL sample of DCF<sup>-</sup> solution (0.65 mM; 195 ppm) was treated with 10 mg of **MOR-1** or **MOR-2** under magnetic stirring for the chosen reaction times. The filtrates from the various reactions were analyzed for their DCF<sup>-</sup> content with UV-Vis.

### 2.5. Preparation of the Column

A glass column (0.7 cm ID column) was partially filled with a mixture of 50 mg of **MOR-1-HA** composite and 5 g of sand (50–70 mesh SiO<sub>2</sub>). As in previous studies [37,38], the column was treated with ~7 mL HCl (4 M) solution and deionized water.

### 2.6. Column Sorption Studies

Several samples of the diclofenac solution (0.07 mM) were passed through the column (flow rate 1 mL min<sup>-1</sup>), collected at the bottom in glass vials and analyzed with UV-Vis. The regeneration of the column-desorption of diclofenac was achieved by its treatment with ~7 mL of HCl acid (4 M) solution. After regeneration, the column was treated with enough water to remove excess acid. The column containing only sand or alginic acid as stationary phase showed no diclofenac sorption capacity.

## 3. Results and Discussion

Our sorption studies involved detailed batch investigations of **MOR-1** and **MOR-2** for removal of DCF<sup>-</sup> including determination of sorption kinetics, sorption isotherms and selectivity vs. common competitive anions. As a second step, the column sorption of DCF<sup>-</sup> by using **MOR-1-HA** composite was investigated in detail. All experiments were performed with solutions of pH = 7 to simulate conditions found in most natural waters [40].

### 3.1. Batch Sorption Studies

#### 3.1.1. Sorption Kinetics

To understand the sorption kinetics, sorption of  $\text{DCF}^-$  by **MOR-1** and **MOR-2** was investigated through variable time sorption experiments. It is evident from Figure 2 that the sorption process for  $\text{DCF}^-$  was outstandingly rapid, as the equilibrium was achieved within 5–6 min for both materials. Interestingly, **MOR-1** removed ~98% of the initial  $\text{DCF}^-$  content ( $\text{DCF}^-$ :  $C_0 = 195$  ppm; 0.65 mM, pH ~6) within only 1 min of contact, respectively, while **MOR-2** removed 96% of  $\text{DCF}^-$  at the same time.

The kinetics data was fitted with the classic kinetic models, i.e., pseudo-first order and pseudo-second order models [41,42], whose mathematical expressions are given below:

$$q_t = q_e[1 - \exp(-K_L t)] \quad (1)$$

$$q_t = \frac{k_2 q_e^2 t}{1 + k_2 q_e t} \quad (2)$$

where  $q_t$  = the amount (mg/g) of ion sorbed by the MOF at different reaction times ( $t$ ),  $q_e$  = the amount ( $\text{mg g}^{-1}$ ) of ion absorbed in equilibrium,  $K_L$  = the Lagergren or first-order rate constant and  $k_2$  is the second-order rate constant [ $\text{g}/(\text{mg}\cdot\text{min})$ ] [42]. The fitting parameters of the above are presented in Table 1. According to the correlation factors ( $R^2$ ), the Ho and Mckay's pseudo-second-order equation could better describe the kinetics data for  $\text{DCF}^-$  sorption by **MOR-1** and **MOR-2** than the pseudo-first-order model, indicating that chemisorption process occurs for  $\text{DCF}^-$  binding [43]. Furthermore, the rate constants (Table 1) indicate faster sorption of  $\text{DCF}^-$  anions by **MOR-1** than **MOR-2**. Presumably, the diffusion of the relatively bulky  $\text{DCF}^-$  anions is facilitated by the larger pores and channels of **MOR-1** (pore sizes for **MOR-1** and **MOR-2** are 0.83–0.88 and 0.55 nm, respectively).

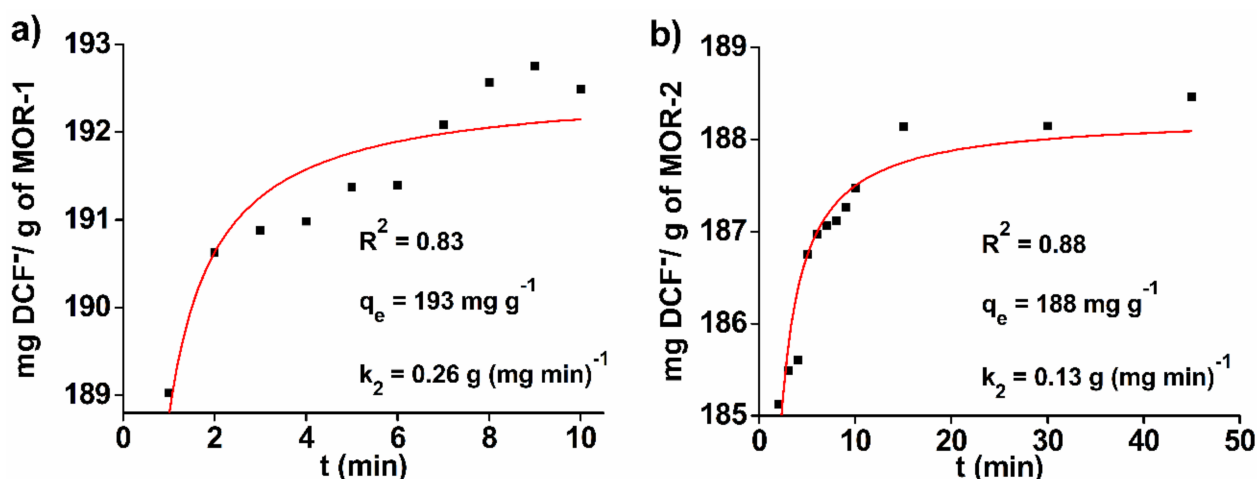


**Figure 2.** Fitting of the kinetics data (solid line) with the Ho–Mckay's second-order equation for the sorption of  $\text{DCF}^-$  by **MOR-1** (a) and **MOR-2** (b).

**Table 1.** Sorption kinetic parameters of **MOR-1** and **MOR-2** for  $\text{DCF}^-$  removal.

Sorbent	Pseudo-First Order Model			Pseudo-Second Order Model		
	$K_L (\text{min}^{-1})$	$q_{e1} (\text{mg g}^{-1})$	$R^2$	$k_2 (\text{g mg}^{-1} \text{min}^{-1})$	$q_{e2} (\text{mg g}^{-1})$	$R^2$
<b>MOR-1</b>	4.26	192	0.5	0.26	192	0.83
<b>MOR-2</b>	2.19	187	0.28	0.13	188	0.88

#### 3.1.2. Sorption Thermodynamics

To better understand the sorption of the pharmaceuticals, we investigated and analyzed the equilibrium data, using the Langmuir, Freundlich, and Langmuir–Freundlich isotherm models. The mathematic expressions of these models are the following [44,45]:

(a) Langmuir

$$q = q_m \frac{bC_e}{1 + bC_e} \quad (3)$$

(b) Freundlich

$$q = K_F C_e^{\frac{1}{n}} \quad (4)$$

(c) Langmuir–Freundlich

$$q = q_m \frac{(bC_e)^{\frac{1}{n}}}{1 + (bC_e)^{\frac{1}{n}}} \quad (5)$$

where  $q$  (mg/g) is the amount of the ion sorbed at the equilibrium concentration  $C_e$  (ppm),  $q_m$  is the maximum sorption capacity of the sorbent,  $b$  (L/mg) is the Langmuir constant related to the free energy of the sorption,  $K_F$  and  $1/n$  are the Freundlich constants. The parameters of Langmuir, Freundlich, and Langmuir–Freundlich (LF) isotherms, found after the fitting of the isotherm  $\text{DCF}^-$  sorption data (Figure 3) are presented in Table 2.

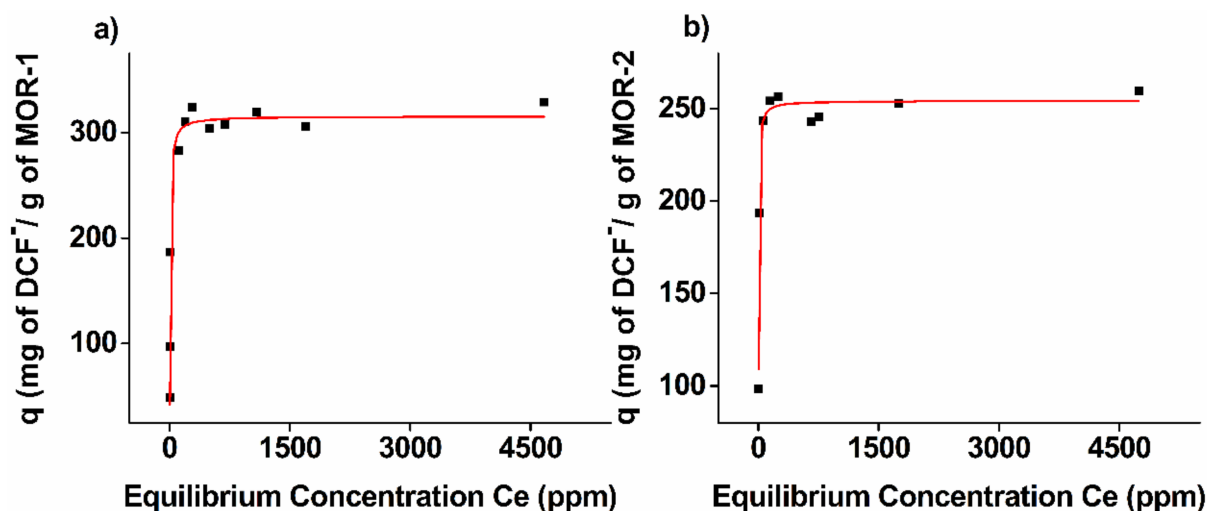


Figure 3. Equilibrium  $\text{DCF}^-$  sorption data for (a) MOR-1 and (b) MOR-2 materials (pH~7). The solid line represents the fitting of the data with the Langmuir model.

Table 2. Modeling parameters for the  $\text{DCF}^-$  removal by MOR-1 and MOR-2.

Sorbent	Langmuir			Freundlich			LF			
	$q_e$ (mg/g)	$b$ (L/mg)	$R^2$	$K_F$ (L/g)	$n$	$R^2$	$q_e$ (mg/g)	$b$ (L/mg)	$n$	$R^2$
MOR-1	$315 \pm 4$	$0.18 \pm 0.02$	0.99	$132 \pm 24$	$7.9 \pm 1.8$	0.76	$318 \pm 5$	$0.17 \pm 0.02$	$1.12 \pm 0.13$	0.99
MOR-2	$254 \pm 3$	$0.4 \pm 0.05$	0.97	$157 \pm 23$	$14 \pm 4.8$	0.57	$252 \pm 3$	$0.39 \pm 0.03$	$0.73 \pm 0.08$	0.99

The isotherm data of  $\text{DCF}^-$  by MOR-1 and MOR-2 can be fitted very well with both Langmuir and LF models, as evidenced by the high  $R^2$  values (>93%). However, the sorption of  $\text{DCF}^-$  by MOR-1 and MOR-2 may be better described by the Langmuir model, as the values of  $1/n$  from the fitting with the LF model were found close to 1. When  $1/n$  values tend to be equal to 1, the LF equation coincides with the Langmuir model. The maximum sorption capacity was calculated to be  $315 \pm 4$  mg of  $\text{DCF}^-$  per g of MOR-1 and  $254 \pm 3$  mg of  $\text{DCF}^-$  per g of MOR-2.

The affinity of the sorbents for the examined pharmaceutical can be described by the distribution coefficient  $K_d$  which is given by the equation:

$$K_d = \frac{V[(C_0 - C_f)/C_f]}{m} \quad (6)$$

where  $C_0$  and  $C_f$  are the initial and equilibrium concentration of the ion (ppm), respectively,  $V$  is the volume (mL) of the testing solution, and  $m$  is the amount of the sorbent (g) used in the experiment. The maximum  $K_d$  values for sorption of  $\text{DCF}^-$  by **MOR-1** and **MOR-2**, obtained from the batch equilibrium studies, were found to be  $1.8 \times 10^5$  and  $5.2 \times 10^4$  mL/g. These values are particularly high and indicate the exceptional affinity of **MOR-1** and **MOR-2** materials for the examined pharmaceutical.

### 3.1.3. Selectivity Studies

The selectivity of **MOR-1** and **MOR-2** for  $\text{DCF}^-$  anions was investigated by performing sorption experiments in the presence of high concentrations of common competitive anions, such as  $\text{Cl}^-$ ,  $\text{NO}_3^-$ , and  $\text{SO}_4^{2-}$ . The  $\text{DCF}^-$  removal efficiency of **MOR-1** and **MOR-2** seems not to be influenced significantly in the presence of 100-fold excess of  $\text{Cl}^-$  or  $\text{NO}_3^-$  anions, with  $\text{DCF}^-$  removal capacities found more than 85% in any case (Figure 4). Interestingly, **MOR-2** removed 92% of the initial  $\text{DCF}^-$  content, even in the presence of 1000-fold excess of  $\text{Cl}^-$ . Moreover, in the presence of competitive  $\text{SO}_4^{2-}$  the ability of both materials to remove  $\text{DCF}^-$  from water was notable, especially for **MOR-2** which can remove 71% of initial  $\text{DCF}^-$  even in the presence of 1000-fold excess of sulfate in the solution. Furthermore, we conducted experiments with  $\text{DCF}^-$  solutions containing simultaneously  $\text{Cl}^-$ ,  $\text{NO}_3^-$ , and  $\text{SO}_4^{2-}$  anions. Likewise, **MOR-1** and **MOR-2** can remove  $\text{DCF}^-$  with only a small decrease in their sorption capability (69% and 78% removal percentages for **MOR-1** and **MOR-2**, respectively). Overall, both **MOR-1** and **MOR-2** materials are proved to be excellent sorbents with significant selectivity for  $\text{DCF}^-$  towards other co-existing anions and, thus, they seem to be very promising candidates for the remediation of real-world wastewater.

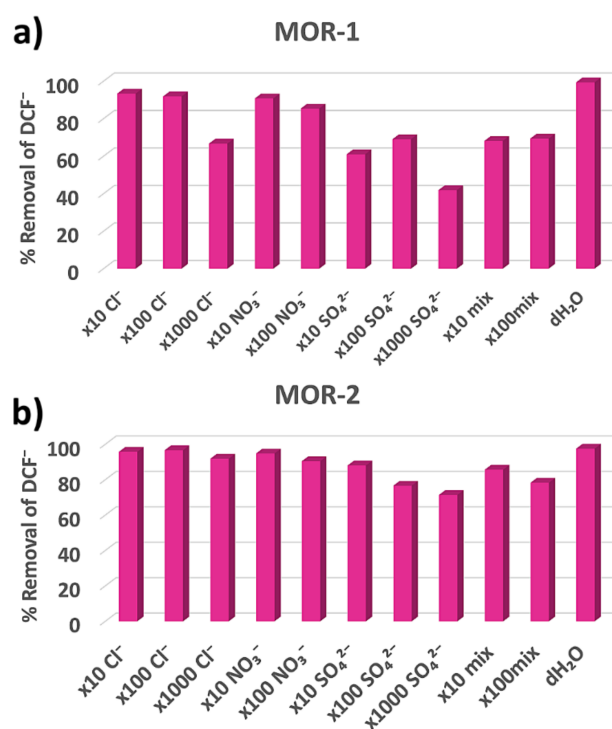


**Figure 4.**  $\text{DCF}^-$  sorption data for (a) **MOR-1** and (b) **MOR-2** in the presence of various competitive anions.

### 3.2. Column Sorption Study

In light of the remarkable sorption capacities of **MOR-1** towards  $\text{DCF}^-$ , we extended our studies to the investigation of the sorption properties under continuous flow conditions. However, pristine **MOR-1** cannot be utilized as stationary phase in columns, considering that this material is isolated as a fine powder and its use in columns results in column clogging or release of the material to the flowing solution. Thus, we utilized the composite form of **MOR-1** with alginic acid (**MOR-1-HA**) [37]. As in our previous studies [37,38,46], the column is filled with a mixture of the **MOF** composite material and silica sand (**MOF** composite:sand mass ratio = 1:100). Column sorption studies were performed with a  $\text{DCF}^-$  solution of initial concentration  $\sim 20$  ppm ( $\text{pH} \sim 7$ ). These investigations revealed that 10 mL of effluent contain no detectable  $\text{DCF}^-$ , whereas relatively high removal capacities ( $>70\%$ ) were observed even after passing 50 mL through the column (Figure 5). The sorbent can be easily regenerated by washing it with  $\text{HCl}$  solution (1.2–4 M). After the regeneration, the column can be reused showing removal capacities close to those of the first run. Even after a third run, the column largely retains its initial sorption capacity.

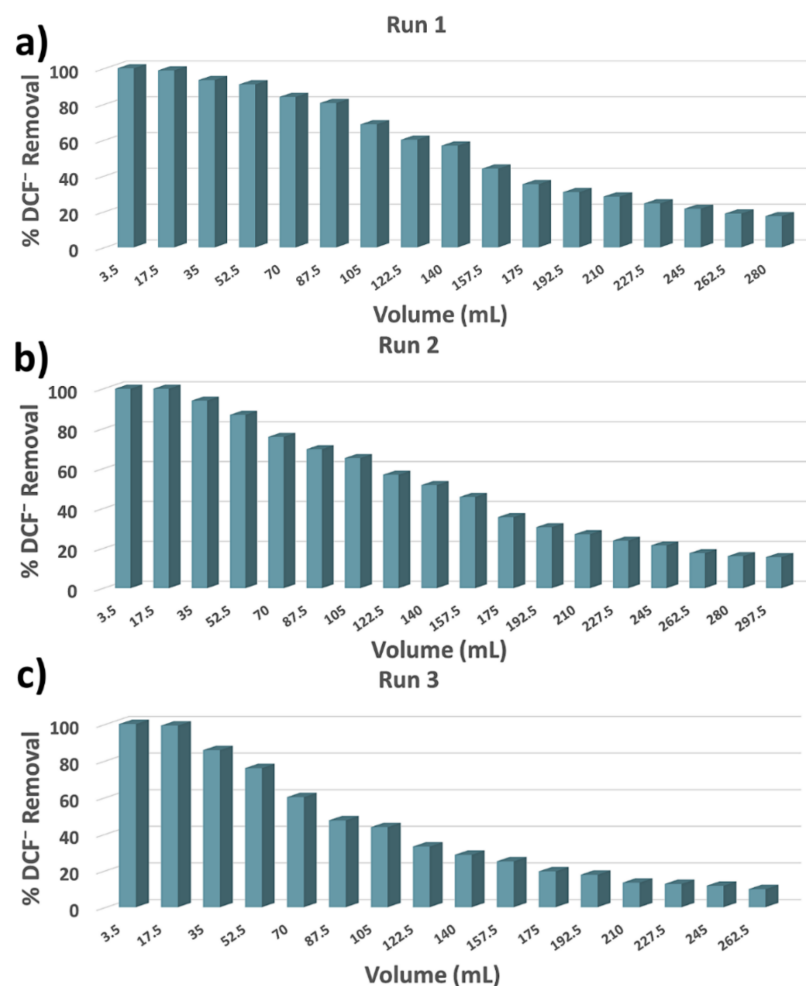


**Figure 5.** (a) The 1st run, (b) 2nd run, and (c) 3rd run of  $\text{DCF}^-$  sorption under continuous flow conditions for **MOR-1-HA** (initial  $\text{DCF}^-$  concentration = 21 ppb).

### 3.3. Characterization of the $\text{DSF}^-$ -Loaded MOFs Mechanism of the $\text{DCF}^-$ Sorption by **MOR-1** and **MOR-2**

The zeta potential of the **MOR-1** and **MOR-2** at  $\text{pH} \sim 7$  was calculated close to zero ( $-0.214$  and  $-0.417$  mV, respectively), indicating neutral surface charge. EDS data further confirmed this evidence since no  $\text{Cl}^-$  was detected for both materials. These results indicate that electrostatic interactions of **MOR-1** and **MOR-2** with  $\text{DCF}^-$  are not likely. Powder X-ray

diffraction (PXRD), unit cell indexing, and Le Bail refinement data for the pharmaceutical-loaded MOFs revealed that the structures of the MOFs were retained after the sorption process (Figure 6).

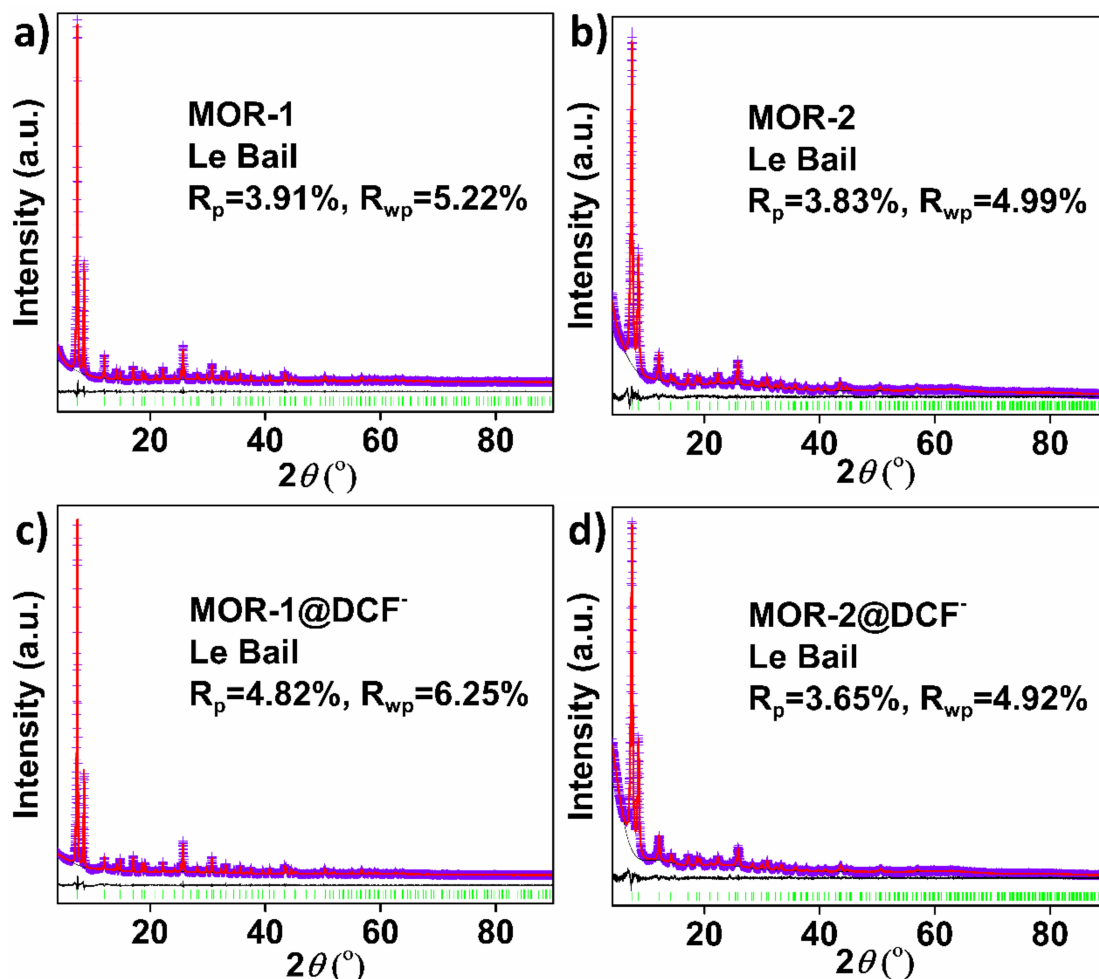


**Figure 6.** Le Bail plot of (a) MOR-1, (b) MOR-2, (c) MOR-1@DCF<sup>-</sup>, and (d) MOR-2@DCF<sup>-</sup>. Cell indexing data from Le Bail refinement: **MOR-1** (space group *Fm-3m*):  $a = 20.785(4)$  Å,  $V = 8979(6)$  Å<sup>3</sup>; **MOR-2** (space group *I<sub>4</sub>/m*):  $a = 14.631(5)$  Å,  $c = 20.743(9)$  Å,  $V = 4441(4)$  Å<sup>3</sup>; **MOR-1@DCF<sup>-</sup>** (space group *Fm-3m*):  $a = 20.771(3)$  Å,  $V = 8962(5)$  Å<sup>3</sup>; **MOR-2@DCF<sup>-</sup>** (space group *I<sub>4</sub>/m*):  $a = 14.59(1)$  Å,  $c = 20.64(1)$  Å,  $V = 4391(9)$  Å<sup>3</sup>. Blue crosses: experimental points; red line, violet crosses: experimental points; red line: calculated pattern; black line: difference pattern (exp-calc); green bars: Bragg positions.

Scanning Electron Microscopy (SEM) images indicate identical morphological characteristics for the pristine MOFs and loaded materials (Figure 7).

FT-IR data for the DCF-loaded MOFs indicated characteristic features of the organic molecules indicating the successful binding of the DCF<sup>-</sup> anions (Figure 8). The most evident change is the appearance of the characteristic band at  $740\text{ cm}^{-1}$  in both **MOR-1@DCF<sup>-</sup>** and **MOR-2@DCF<sup>-</sup>** spectra, corresponding to the C-Cl stretching [47]. Furthermore, the changes observed in the region from  $3500$  to  $3300\text{ cm}^{-1}$  are attributed to the N-H stretching of the secondary amines. In addition, both spectra display a slight shift of the C=O stretching band from  $1568$  to  $1573\text{ cm}^{-1}$  (**MOR-1**) and from  $1571$  to  $1576\text{ cm}^{-1}$  (**MOR-2**) after the DCF<sup>-</sup> sorption process, suggesting the participation of the carboxylic acid groups in DCF<sup>-</sup> sorption [47].

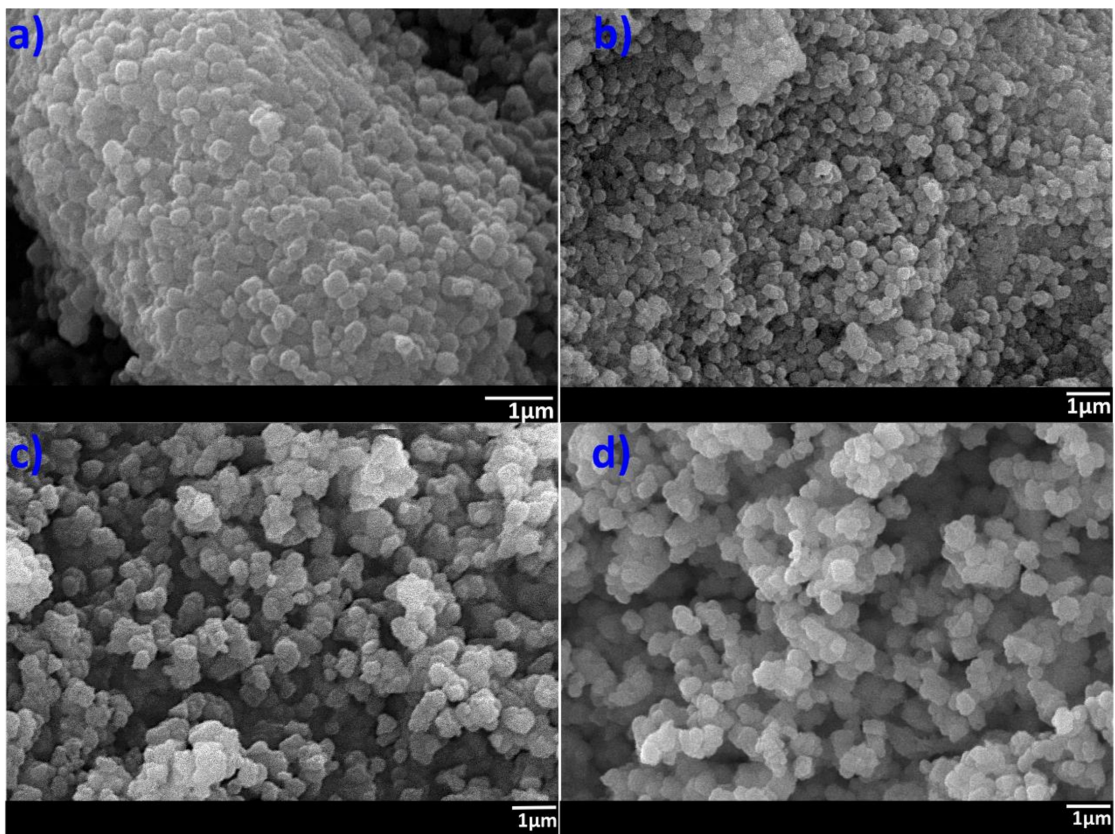


Figure 7. SEM images of (a) MOR-1, (b) MOR-2, (c) MOR-1@DCF<sup>-</sup>, and (d) MOR-2@DCF<sup>-</sup>.

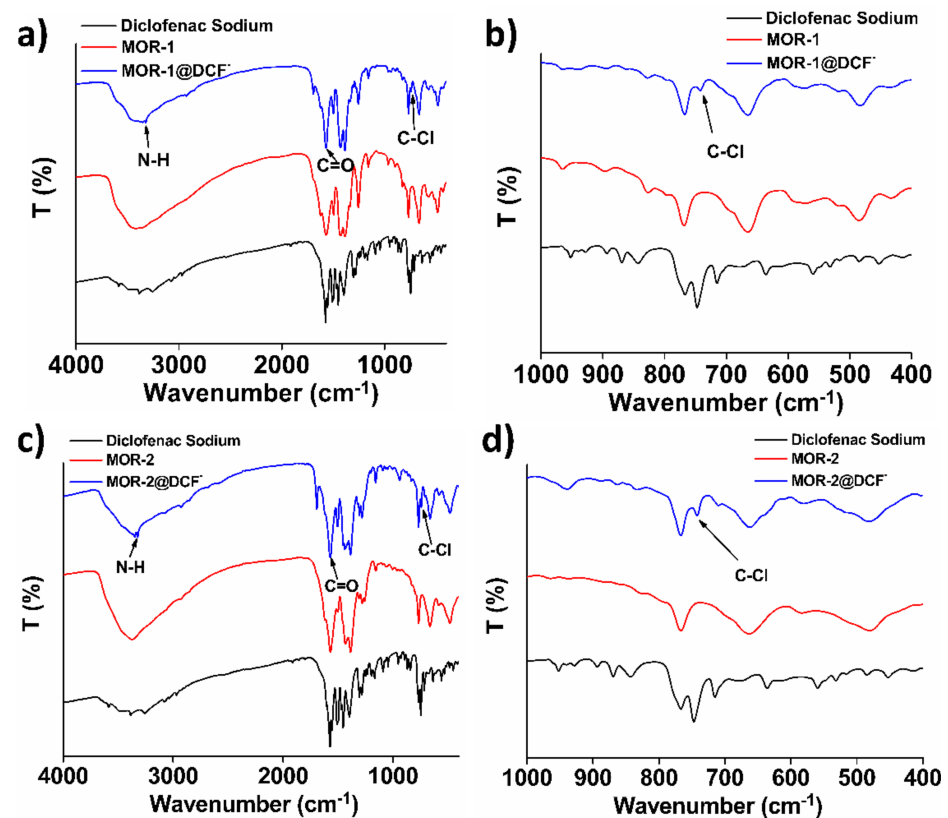


Figure 8. ATR-IR spectra of diclofenac sodium salt, (a,b) MOR-1, MOR-1@DCF<sup>-</sup>, and (c,d) MOR-2, MOR-2@DCF<sup>-</sup>.

Based on the above characterization data and sorption results, we conclude that  $\text{DCF}^-$  anions are likely ligated to  $\text{Zr}^{4+}$  centers of **MOR-1** and **MOR-2**, presumably via their  $\text{COO}^-$  groups. Thus, the mechanism of sorption may involve replacement of terminal  $\text{OH}/\text{H}_2\text{O}$  groups (e.g., **MOR-2** contains 8 terminal  $\text{OH}/\text{H}_2\text{O}$  groups per  $\text{Zr}_6$  cluster) by  $\text{DCF}^-$  anions (Figure 9). **MOR-1** has sufficiently large pores (0.83–0.88 nm) to host  $\text{DCF}^-$  having a diameter of about 0.83 nm (Figure 1). The insertion of  $\text{DCF}^-$  into the pores of the **MOR-1** is further consistent with the significantly reduced BET surface area of **MOR-1@DCF<sup>-</sup>** (557  $\text{m}^2/\text{g}$ ) in comparison to that of pristine **MOR-1** (1097  $\text{m}^2/\text{g}$ ) (Figure 10). In contrast, the small pore dimensions of **MOR-2** (0.55 nm) likely restrict the entrance of  $\text{DCF}^-$  into the voids of the MOF and the sorption of  $\text{DCF}^-$  by **MOR-2** may occur predominantly on the external surface. Still, the BET surface area of **MOR-2@DSF<sup>-</sup>** (214  $\text{m}^2/\text{g}$ ) is significantly smaller than that of **MOR-2** (354  $\text{m}^2/\text{g}$ ) (Figure 10).

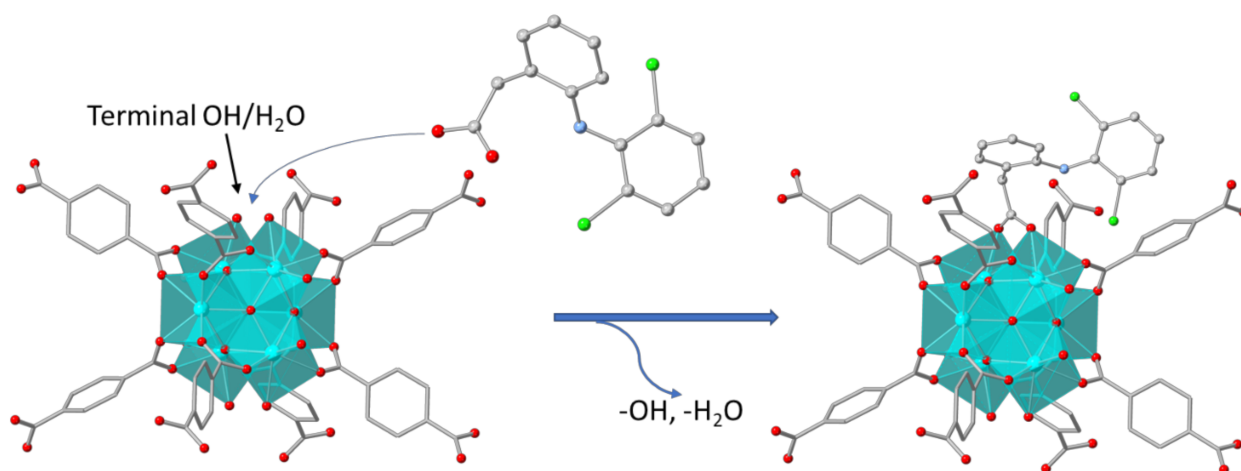


Figure 9. Suggested mechanism for the capture of  $\text{DCF}^-$  by **MOR-1/MOR-2**.

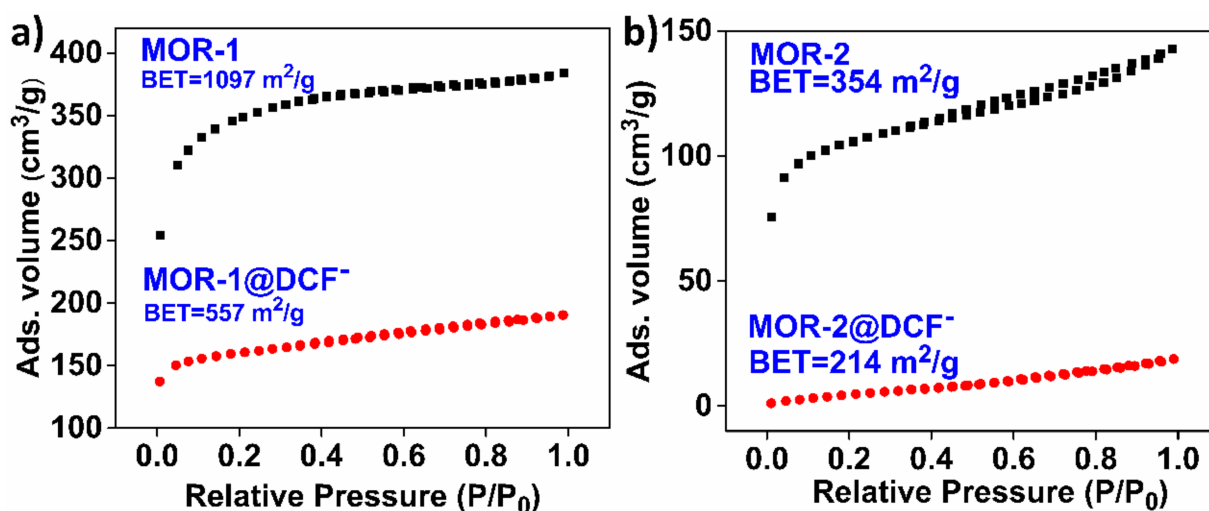


Figure 10.  $\text{N}_2$  adsorption isotherms (77 K) for (a) **MOR-1**, **MOR-1@DCF<sup>-</sup>**, and (b) **MOR-2**, **MOR-2@DCF<sup>-</sup>**.

### 3.4. Comparison of **MOR-1** and **MOR-2** with Other MOF-Based Sorbents

In Table 3, we present selected  $\text{DCF}^-$  sorption characteristics of various MOF-based sorbents in neutral aqueous media and compare them with those of the **MOR-1** and **MOR-2**. Most of these sorbents display maximum sorption capacities much higher than those of our materials. However, in most cases the equilibrium is achieved after long stirring periods, which is a significant drawback for real applications requiring instant removal of

pollutants from aqueous media. In contrast, **MOR-1** and **MOR-2** show the fastest sorption kinetics among MOF-based sorbents with equilibrium times of only 5–6 min. Another important feature that both **MOR-1** and **MOR-2** display is their capability to remove DCF<sup>−</sup> satisfactorily under antagonistic conditions commonly encountered in natural waters. Such studies for reported MOF-based sorbents are scarce. However, the critical point of this study is the utilization of **MOR-1** in an ion sorption column. To the best of our knowledge, **MOR-1** is the first MOF with demonstrated sorption capability for DCF<sup>−</sup> under flow conditions, offering a great opportunity for further applications in the field of real waste remediation.

**Table 3.** Comparison of the sorption characteristics of **MOR-1** and **MOR-2** with those of other MOF-based sorbents.

MOF-Based Sorbent	Capacity mg/g	Equilibrium Time	Selectivity vs.	Reusability	Column Study	Ref.
Fe <sub>3</sub> O <sub>4</sub> @MIL-100(Fe)	400	250 min	NA	NA	NA	[29]
[Cu(BTTA)] <sub>n</sub> •2DMF	650	450 min	NA	Reusable	NA	[30]
Magnetic GO/ZIF-8/g-AIOOH-NC	2594.3	50 min	NA	Reusable	NA	[31]
Defective UiO-66	321	120 min	Various pharmaceutical pollutants	NA	NA	[32]
MOF-808	833	5 h	NA	NA	NA	[33]
Fe <sub>3</sub> O <sub>4</sub> @MOF-100(Fe)	377.36	24 h	NA	Reusable	NA	[34]
<b>MOR-1</b>	<b>315</b>	<b>5 min</b>	Cl <sup>−</sup> , NO <sub>3</sub> <sup>−</sup> , SO <sub>4</sub> <sup>2−</sup>	<b>Reusable</b>	<b>3 runs</b>	<b>This work</b>
<b>MOR-2</b>	<b>254</b>	<b>5 min</b>	Cl <sup>−</sup> , NO <sub>3</sub> <sup>−</sup> , SO <sub>4</sub> <sup>2−</sup>	<b>Reusable</b>	<b>NA</b>	<b>This work</b>

#### 4. Conclusions

In conclusion, we reported the detailed DCF<sup>−</sup> batch sorption studies of **MOR-1** and **MOR-2**. These materials displayed fast sorption kinetics (equilibrium time ~5–6 min) and satisfying removal capacities. Interestingly, the kinetics conducted in this study revealed the fastest DCF<sup>−</sup> sorption processes by MOFs ever reported. At the same time, **MOR-1** and **MOR-2** have shown noticeably selective sorption towards DCF<sup>−</sup> in aqueous samples containing a variety of coexisting anions, which reveals that these materials may be suitable for real world applications. It is worth emphasizing that **MOR-1**, in its composite form with alginic acid, is the first MOF used in a sorption column for elimination of pharmaceuticals and was found highly efficient for the removal of DCF<sup>−</sup> from contaminated aqueous solutions. Overall, the present study indicates that MOF-based sorbents are promising for the removal of pharmaceuticals under realistic conditions and for practical water treatment requiring continuous flow. Efforts to develop more effective MOF and MOF-composite sorbents for capture of pharmaceuticals from aqueous media are underway in our laboratory.

**Author Contributions:** Investigation, A.D.P., E.K.A. and G.S.A.; data curation, A.D.P., E.K.A. and G.S.A.; writing—original draft, A.D.P.; conceptualization, M.J.M.; writing—review and editing, M.J.M.; supervision, M.J.M. All authors have read and agreed to the published version of the manuscript.

**Funding:** The research work was supported by the Hellenic Foundation for Research and Innovation (H.F.R.I.) under the “First Call for H.F.R.I. Research Projects to support Faculty members and Researchers and the procurement of high-cost research equipment grant” (Project Number: 348).

**Data Availability Statement:** All data in this study are provided in the present manuscript.

**Conflicts of Interest:** The authors declare no conflict of interest.

## References

1. Daughton, C.G.; Ternes, T.A. Pharmaceuticals and personal care products in the environment: Agents of subtle change? *Environ. Health Perspect.* **1999**, *107*, 907–938. [[CrossRef](#)] [[PubMed](#)]
2. Wang, J.; Wang, S. Removal of pharmaceuticals and personal care products (PPCPs) from wastewater: A review. *J. Environ. Manag.* **2016**, *82*, 620–640. [[CrossRef](#)] [[PubMed](#)]
3. Sahoo, P. The adverse effects of estrogenic pill driven after flexible fertility on environment in covid-19 situation. *Eng. Sci.* **2021**, *14*, 109–113. [[CrossRef](#)]
4. Akhtar, J.; Amin, N.A.S.; Shahzad, K. A review on removal of pharmaceuticals from water by adsorption. *Desalin. Water Treat.* **2016**, *57*, 12842–12860. [[CrossRef](#)]
5. Petrie, B.; Barden, R.; Kasprzyk-Hordern, B. A review on emerging contaminants in wastewaters and the environment: Current knowledge, understudied areas and recommendations for future monitoring. *Water Res.* **2015**, *72*, 3–27. [[CrossRef](#)] [[PubMed](#)]
6. Kümmerer, K. The presence of pharmaceuticals in the environment due to human use—Present knowledge and future challenges. *J. Environ. Manag.* **2009**, *90*, 2354–2366. [[CrossRef](#)]
7. Mompelat, S.; Le Bot, B.; Thomas, O. Occurrence and fate of pharmaceutical products and by-products, from resource to drinking water. *Environ. Int.* **2009**, *35*, 803–814. [[CrossRef](#)]
8. Heberer, T. Tracking persistent pharmaceutical residues from municipal sewage to drinking water. *J. Hydrol.* **2002**, *266*, 175–189. [[CrossRef](#)]
9. Wieszczycka, K.; Zembruska, J.; Bornikowska, J.; Wojciechowska, A.; Wojciechowska, I. Removal of naproxen from water by ionic liquid-modified polymer sorbents. *Chem. Eng. Res. Des.* **2017**, *117*, 698–705. [[CrossRef](#)]
10. Tang, Y.; Li, X.M.; Xu, Z.C.; Guo, Q.W.; Hong, C.Y.; Bing, Y.X. Removal of naproxen and bezafibrate by activated sludge under aerobic conditions: Kinetics and effect of substrates. *Biotechnol. Appl. Biochem.* **2014**, *61*, 333–341. [[CrossRef](#)]
11. Rivera-Jiménez, S.M.; Méndez-González, S.; Hernández-Maldonado, A. Metal (M = Co<sup>2+</sup>, Ni<sup>2+</sup>, and Cu<sup>2+</sup>) grafted mesoporous SBA-15: Effect of transition metal incorporation and pH conditions on the adsorption of Naproxen from water. *Microporous Mesoporous Mater.* **2010**, *132*, 470–479. [[CrossRef](#)]
12. Boyd, G.R.; Reemtsma, H.; Grimm, D.A.; Mitra, S. Pharmaceuticals and personal care products (PPCPs) in surface and treated waters of Louisiana, USA and Ontario, Canada. *Sci. Total Environ.* **2003**, *311*, 135–149. [[CrossRef](#)]
13. Joss, A.; Zabczynski, S.; Göbel, A.; Hoffmann, B.; Löffler, D.; McArdell, C.S.; Ternes, T.A.; Thomsen, A.; Siegrist, H. Biological degradation of pharmaceuticals in municipal wastewater treatment: Proposing a classification scheme. *Water Res.* **2006**, *40*, 1686–1696. [[CrossRef](#)] [[PubMed](#)]
14. Zwiener, C.; Frimmel, F.H. Short-term tests with a pilot sewage plant and biofilm reactors for the biological degradation of the pharmaceutical compounds clofibric acid, ibuprofen, and diclofenac. *Sci. Total Environ.* **2003**, *309*, 201–211. [[CrossRef](#)]
15. Buser, H.R.; Poiger, T.; Müller, M.D. Occurrence and fate of the pharmaceutical drug diclofenac in surface waters: Rapid photodegradation in a lake. *Environ. Sci. Technol.* **1998**, *32*, 3449–3456. [[CrossRef](#)]
16. Boyd, G.R.; Zhang, S.; Grimm, D.A. Naproxen removal from water by chlorination and biofilm processes. *Water Res.* **2005**, *39*, 668–676. [[CrossRef](#)]
17. Hasan, Z.; Khan, N.A.; Jhung, S.H. Adsorptive removal of diclofenac sodium from water with Zr-based metal–organic frameworks. *Chem. Eng. J.* **2016**, *284*, 1406–1413. [[CrossRef](#)]
18. Song, J.Y.; Jhung, S.H. Adsorption of pharmaceuticals and personal care products over metal-organic frameworks functionalized with hydroxyl groups: Quantitative analyses of H-bonding in adsorption. *Chem. Eng. J.* **2017**, *322*, 366–374. [[CrossRef](#)]
19. Hasan, Z.; Jeon, J.; Jhung, S.H. Adsorptive removal of naproxen and clofibric acid from water using metal-organic frameworks. *J. Hazard. Mater.* **2012**, *209–210*, 151–157. [[CrossRef](#)]
20. Ahmed, M.B.; Zhou, J.L.; Ngo, H.H.; Guo, W. Adsorptive removal of antibiotics from water and wastewater: Progress and challenges. *Sci. Total Environ.* **2015**, *532*, 112–126. [[CrossRef](#)]
21. Flores-Cano, J.V.; Sánchez-Polo, M.; Messoud, J.; Velo-Gala, I.; Ocampo-Pérez, R.; Rivera-Utrilla, J. Overall adsorption rate of metronidazole, dimetridazole and diatrizoate on activated carbons prepared from coffee residues and almond shells. *J. Environ. Manag.* **2016**, *169*, 116–125. [[CrossRef](#)] [[PubMed](#)]
22. Méndez-Díaz, J.D.; Prados-Joya, G.; Rivera-Utrilla, J.; Leyva-Ramos, R.; Sánchez-Polo, M.; Ferro-García, M.A.; Medellín-Castillo, N.A. Kinetic study of the adsorption of nitroimidazole antibiotics on activated carbons in aqueous phase. *J. Colloid Interface Sci.* **2010**, *345*, 481–490. [[CrossRef](#)] [[PubMed](#)]
23. Rivera-Jiménez, S.M.; Hernández-Maldonado, A.J. Nickel (II) grafted MCM-41: A novel sorbent for the removal of Naproxen from water. *Microporous Mesoporous Mater.* **2008**, *116*, 246–252. [[CrossRef](#)]
24. Domínguez, J.R.; González, T.; Palo, P.; Cuerda-Correa, E.M. Removal of common pharmaceuticals present in surface waters by Amberlite XAD-7 acrylic-ester-resin: Influence of pH and presence of other drugs. *Desalination* **2011**, *269*, 231–238. [[CrossRef](#)]
25. Rahardjo, A.K.; Susanto, M.J.J.; Kurniawan, A.; Indraswati, N.; Ismadji, S. Modified Ponorogo bentonite for the removal of ampicillin from wastewater. *J. Hazard. Mater.* **2011**, *190*, 1001–1008. [[CrossRef](#)]

26. Eddaoudi, M.; Moler, D.B.; Li, H.; Chen, B.; Reineke, T.M.; O’Keeffe, M.; Yaghi, O.M. Modular Chemistry: Secondary Building Units as a Basis for the Design of Highly Porous and Robust Metal–Organic Carboxylate Frameworks. *Acc. Chem. Res.* **2001**, *34*, 319–330. [[CrossRef](#)]
27. Horike, S.; Shimomura, S.; Kitagawa, S. Soft porous crystals. *Nat. Chem.* **2009**, *1*, 695–704. [[CrossRef](#)]
28. Férey, G. Hybrid porous solids: Past, present, future. *Chem. Soc. Rev.* **2008**, *37*, 191–214. [[CrossRef](#)]
29. Li, S.; Cui, J.; Wu, X.; Zhang, X.; Hu, Q.; Hou, X. Rapid in situ microwave synthesis of Fe<sub>3</sub>O<sub>4</sub>@MIL-100(Fe) for aqueous diclofenac sodium removal through integrated adsorption and photodegradation. *J. Hazard. Mater.* **2019**, *373*, 408–416. [[CrossRef](#)]
30. Liu, W.; Shen, X.; Han, Y.; Liu, Z.; Dai, W.; Dutta, A.; Kumar, A.; Liu, J. Selective adsorption and removal of drug contaminants by using an extremely stable Cu (II)-based 3D metal-organic framework. *Chemosphere* **2019**, *215*, 524–531. [[CrossRef](#)]
31. Arabkhani, P.; Javadian, H.; Asfaram, A.; Ateia, M. Decorating graphene oxide with zeolitic imidazolate framework (ZIF-8) and pseudo-boehmite offers ultra-high adsorption capacity of diclofenac in hospital effluents. *Chemosphere* **2021**, *271*, 129610. [[CrossRef](#)] [[PubMed](#)]
32. Zhuang, S.; Wang, J. Adsorptive removal of pharmaceutical pollutants by defective metal organic framework UiO-66: Insight into the contribution of defects. *Chemosphere* **2021**, *281*, 130997. [[CrossRef](#)] [[PubMed](#)]
33. Prasetya, N.; Li, K. MOF-808 and its hollow fibre adsorbents for efficient diclofenac removal. *Chem. Eng. J.* **2021**, *417*, 129216. [[CrossRef](#)]
34. Yu, S.; Wan, J.; Chen, K. A facile synthesis of superparamagnetic Fe<sub>3</sub>O<sub>4</sub> supraparticles@MIL-100(Fe) core-shell nanostructures: Preparation, characterization and biocompatibility. *J. Colloid Interface Sci.* **2016**, *461*, 173–178. [[CrossRef](#)] [[PubMed](#)]
35. Huang, L.; Shen, R.; Shuai, Q. Adsorptive removal of pharmaceuticals from water using metal-organic frameworks: A review. *J. Environ. Manag.* **2021**, *277*, 111389. [[CrossRef](#)] [[PubMed](#)]
36. Tchobanoglous, G.; Burton, F.L.; dan Stensel, H.D. *Waste Water Engineering: Treatment and Reuse*, 4th ed.; Metcalf & Eddy, Inc.: Boston, MA, USA, 2003.
37. Rapti, S.; Pournara, A.; Sarma, D.; Papadas, I.T.; Armatas, G.S.; Tsipis, A.C.; Lazarides, T.; Kanatzidis, M.G.; Manos, M.J. Selective capture of hexavalent chromium from an anion-exchange column of metal organic resin–alginate composite. *Chem. Sci.* **2016**, *7*, 2427–2436. [[CrossRef](#)]
38. Rapti, S.; Sarma, D.; Diamantis, S.A.; Skliri, E.; Armatas, G.S.; Tsipis, A.C.; Hassan, Y.S.; Alkordi, M.; Malliakas, C.D.; Kanatzidis, M.G.; et al. All in one porous material: Exceptional sorption and selective sensing of hexavalent chromium by using a Zr<sup>4+</sup> MOF. *J. Mater. Chem. A* **2017**, *5*, 14707–14719. [[CrossRef](#)]
39. Coelho, A.A. TOPAS and TOPAS-Academic: An optimization program integrating computer algebra and crystallographic objects written in C++. *J. Appl. Crystallogr.* **2018**, *51*, 210–218. [[CrossRef](#)]
40. Wilkinson, J.L.; Boxall, A.B.A.; Kolpin, D.W.; Leung, K.M.Y.; Lai, R.W.S.; Galban-Malag, C.; Adell, A.D.; Mondon, J.; Metian, M.; Marchant, R.A.; et al. Pharmaceutical pollution of the world’s rivers. *Proc. Natl. Acad. Sci. USA* **2022**, *119*, e2113947119. [[CrossRef](#)]
41. Ho, Y.S.; McKay, G. Pseudo-second order model for sorption processes. *Process Biochem.* **1999**, *34*, 451–465. [[CrossRef](#)]
42. Benhammou, A.; Yaacoubi, A.; Nibou, L.; Tanouti, B. Adsorption of metal ions onto Moroccan stevensite: Kinetic and isotherm studies. *J. Colloid Interface Sci.* **2005**, *282*, 320–326. [[CrossRef](#)] [[PubMed](#)]
43. Godiya, C.B.; Kumar, S.; Xiao, Y. Amine functionalized egg albumin hydrogel with enhanced adsorption potential for diclofenac sodium in water. *J. Hazard. Mater.* **2020**, *393*, 122417. [[CrossRef](#)] [[PubMed](#)]
44. Manos, M.J.; Kanatzidis, M.G. Sequestration of heavy metals from water with layered metal sulfides. *Chem. A Eur. J.* **2009**, *15*, 4779–4784. [[CrossRef](#)] [[PubMed](#)]
45. Manos, M.J.; Ding, N.; Kanatzidis, M.G. Layered metal sulfides: Exceptionally selective agents for radioactive strontium removal. *Proc. Natl. Acad. Sci. USA* **2008**, *105*, 3696–3699. [[CrossRef](#)] [[PubMed](#)]
46. Rapti, S.; Pournara, A.; Sarma, D.; Papadas, I.T.; Armatas, G.S.; Hassan, Y.S.; Alkordi, M.H.; Kanatzidis, M.G.; Manos, M.J. Rapid, green and inexpensive synthesis of high quality UiO-66 amino-functionalized materials with exceptional capability for removal of hexavalent chromium from industrial waste. *Inorg. Chem. Front.* **2016**, *3*, 635–644. [[CrossRef](#)]
47. Sun, K.; Shi, Y.; Wang, X.; Rasmussen, J.; Li, Z.; Zhu, J. Organokaolin for the uptake of pharmaceuticals diclofenac and chloramphenicol from water. *Chem. Eng. J.* **2017**, *330*, 1128–1136. [[CrossRef](#)]